Title
Ventilation, thermal and luminous autonomy metrics for an integrated design process

Authors
Ko, Won Hee
Schiavon, Stefano
Brager, Gail
et al.

Publication Date
2018-11-01

DOI
10.1016/j.buildenv.2018.08.038

Peer reviewed

Ventilation, Thermal and Luminous Autonomy Metrics for an Integrated Design Process

Won Hee Ko[1*], Stefano Schiavon[1], Gail Brager[1], Brendon Levitt[2]

[1]Center for the Built Environment, University of California, Berkeley, USA

[2]Loisos + Ubbelohde, Alameda, California, USA

* Corresponding author:

E-mail address: wonheeko@berkeley.edu

Address: 390 Wurster Hall, Berkeley, CA 94720-1839, USA

Abstract

This paper proposes and evaluates an integrated workflow that simultaneously uses ventilation, thermal, and luminous autonomy for the assessment of passive design strategies, introducing a potential way to integrate these three metrics in the design process. We developed a new metric, ventilation autonomy, and assessed the advantages and limitations of applying the three autonomy metrics with building performance simulations in two climates. We developed a novel visualization to display the hourly and yearly environmental autonomy values. The results show that when we consider the three metrics together, designers may have contradicting design directions if trying to both mitigate the solar radiation and to utilize natural ventilation. The visualizations that categorize nine combinations of thermal and visual comfort along with ventilation autonomy are effective in showing the trade-offs among ventilation, thermal, and visual performance.

Keywords

Building autonomy, thermal comfort, visual comfort, ventilation autonomy, integrated design, resilience

Graphical Abstract

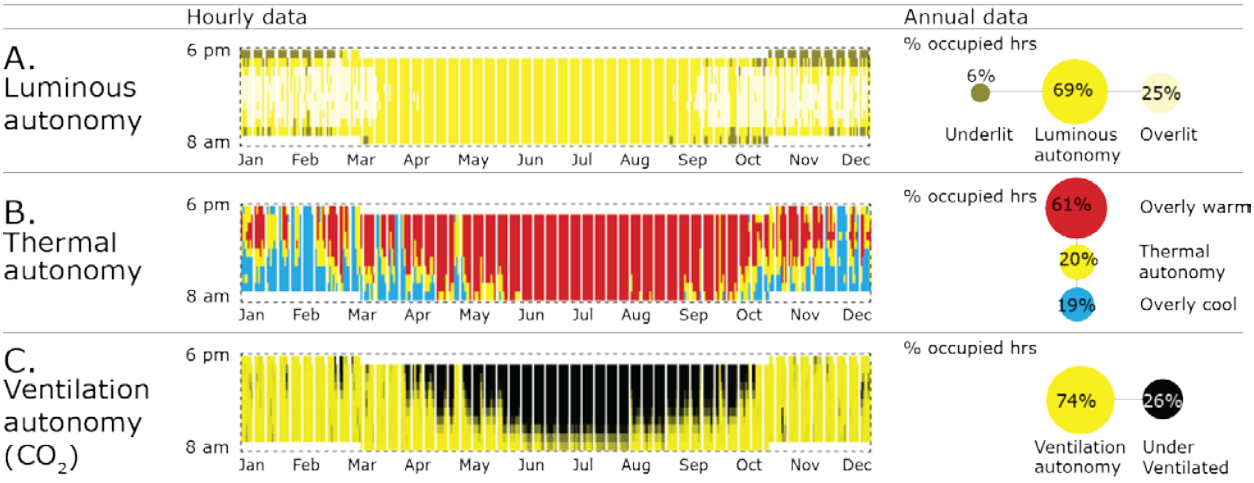

https://doi.org/10.1016/j.buildenv.2018.08.038
http://escholarship.org/uc/item/81t2t9vd

1. Introduction

An autonomous building is a building that can function independently without support or services from public facilities [1]. It combines energy conservation/generation, and passive design to maintain a comfortable environment [2]. With the increasing number of climate-related events causing property damage [3], the concept of passive survivability has received increased attention within the building industry [4,5]. The term passive survivability describes a building's ability to maintain critical life-support conditions in the event of extended loss of power with minimal external input, by maximizing the utilization of natural heating/cooling, lighting, and ventilation [6]. In order to design an autonomous building that supports passive survivability, the building envelope must be designed and controlled in a way that achieves a high level of environmental autonomy (i.e., with ventilation, thermal and luminous autonomy). Considering environmental autonomy in the building design process encourages designers to focus on how building design performs independent of mechanical and lighting systems [7]. As a consequence, it helps the designers understand the relationship between the building envelope and the occupants' comfort. It clearly differs from most building performance metrics that were developed to inform the design of mechanical systems or to minimize energy use.

One of the primary design goals for environmental autonomy is to simultaneously create comfortable conditions while maintaining high levels of energy efficiency. The understanding of the integrated effect of building performance criteria (i.e., luminous, thermal and air quality) is critical to achieve a high level of environmental autonomy. However, these three metrics are at very different stages of development. Among the three, the concept of luminous autonomy is relatively well understood, and refers to the percentage of occupied time over a year in which daylight levels meet the required lighting range for a space [8]. In comparison, thermal autonomy is a relatively new concept, and is defined as the percentage of occupied time over a year where a thermal zone meets a given set of thermal comfort criteria through passive means only [7,9]. The concept of autonomy regarding indoor air quality is not yet developed at all, and we define it here for the first time regarding ventilation. We propose that ventilation autonomy should represent the percentage of occupied hours over a year in which a minimum ventilation rate can be achieved by natural ventilation only.

2. Integrated effect of indoor environmental quality and current research gap

Integrated design is the process encompassing cross-disciplinary teamwork that improves integration of building [10,11] and it is a key to sustainable design that should be addressed in the very early design stage [12]. Despite the advances in simulations tools and building data [13–17], several research gaps could address integrated design, especially the integrated effect of the IEQ on people.

First, researchers have rarely investigated three indoor environmental quality (IEQ) *physical* factors (i.e., lighting, thermal, and indoor air quality) together [18]. Some researchers have assessed two out of the three indoor environmental quality metrics (e.g., lighting and thermal) for integrated design [19–21]. Others have focused on the simultaneous evaluation of one or two physical factors and energy performance [22–26].

Second, building performance metrics focusing on *occupants' comfort* to multiple environmental variables are still lacking as well. For example, balancing solar gain scarcity and surplus regarding window heat transfer and building energy use is well-established in passive design [17], but the effect of windows on occupants' comfort and well-being has not yet been fully assessed. Some researchers have studied window performance for thermal comfort [27–33]. Others

have focused on the impact of daylight and view through windows on occupants' visual comfort and well-being [34–37]. However, only a few studies have proposed guidelines or examples for developing comfort-based, occupant-centric building performance metrics [38,39]. These are either broad concept level work (i.e., the metrics have not reached maturity to be integrated into the design process) or limited to two indoor environmental quality metrics only (e.g., visual and thermal aspects).

Lastly, there is a need for compelling visualization methods that simultaneously compare the impact of a building design on all three IEQ factors. In practice, engineers generally make different models for specific purposes (e.g., parallel thermal and daylight models, shown symbolically in Figure 1) and then try to compare the disconnected results. This separate modeling and visualization process make it difficult for designers and engineers to understand the trade-offs regarding how a single decision about the building envelope design or control impacts multiple environmental quality factors, and the subsequent effect on occupants' overall comfort and experience in the building. The visualizations that consider a specific environmental quality may convey more detailed information. However, an integrated visualization method can address the simultaneous impact of the design decisions on the multiple environmental conditions. Improved data visualizations can lead to a better integration that supports more comfortable, sustainable and resilient buildings.

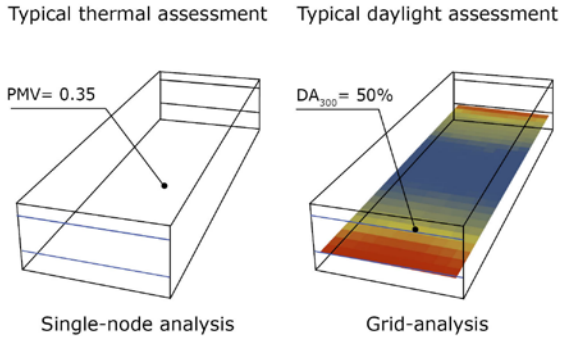

Figure 1: *Typical outputs from thermal and daylight assessments.*

To overcome the research gaps listed above, this paper proposes a novel workflow that simultaneously evaluates luminous, thermal, and ventilation autonomy for integrated building design. Towards this end, we performed three steps: 1) develop, define and assess ventilation autonomy metric, 2) develop a workflow and data visualizations for understanding the trade-offs and interactions among luminous, thermal, and ventilation autonomy, and 3) assess the proposed method by testing the impact of internal shading and operable window systems in a simple building located in two climates. The proposed workflow and visualizations may help building professionals consider the compromises in their decision-making processes by providing a better understanding of the interactions, trade-offs, and synergies between these three IEQ factors.

3. Building autonomy theory and metrics

3.1 Luminous autonomy

Luminous autonomy metrics have minimum and maximum threshold values that define the proper amount of daylight respectively as sufficient but not excessive. Most daylight sufficiency metrics use minimum illuminance to define the threshold, which is typically the IES recommendation for a given task type [40]. Among various luminous metrics, Daylight Autonomy

(DA) is most commonly used to determine the percentage of the occupied hours of the year when the minimum illuminance requirement (e.g., 300 lux for an office environment) at a sensor is met by daylight alone [41]. It is defined by the following equation:

$$DA = \frac{\sum_{i=1}^{N_t}(wf_i \cdot t_i)}{\sum_{i=1}^{N_t}(t_i)} \in [0,1] \text{ with } wf_i = \begin{cases} 1 \text{ if } I_{avail} \geq I_{limit} \\ 0 \text{ if } I_{avail} < I_{limit} \end{cases} \quad (1)$$

where, t_i represents occupied hours, N_t is the number of time steps, I_{avail} is the available daylight level, I_{limit} is the illuminance threshold, and wf_i is a weighting factor depending on the illuminance threshold.

Spatial Daylight Autonomy (sDA) is a metric describing annual sufficiency of ambient daylight levels in a spatial format. It is defined as the percentage of an analysis area that meets a minimum daylight illuminance level for a specified fraction of the operating hours per year. Lighting standard LM-83-12 [8] has introduced sDA as the metric for daylight sufficiency. It also requires that the effect of shades be included in sDA calculations.

For the maximum daylight threshold, there are a few metrics evaluating visual discomfort or glare caused by excessive daylight. These maximum threshold metrics include Annual Sunlight Exposure (ASE), which is based on horizontal illuminance, and Daylight Glare Index (DGI) or Daylight Glare Probability (DGP), which is based on luminance. Lighting standard LM-83-12 [8] uses ASE as a proxy for evaluating the potential for glare; it is the percentage of an analysis area that exceeds a specified direct sunlight illuminance level (typically 1,000 lux) for more than a specified number of hours per year. It is arguably the case that luminance-based glare metrics (such as DGI and DGP) are more likely to correlate with the subjective assessment of visual comfort in office environments than illuminance-based metrics [42,43]. However, luminance-based glare metrics require a detailed level of indoor and outdoor information (e.g., desk layout for view angles) that designers may not know in the early design phase. In addition, they also require a higher computational analysis. Several researchers claim that none of the glare metrics accurately predict visual discomfort [44–46].

Useful Daylight Illuminance (UDI) is another luminous autonomy metric [47] that combines both the minimum and maximum thresholds by using horizontal illuminance calculations. The UK Education Funding Agency's Priority Schools Building Programme uses UDI to measure adequate daylight levels for new schools [48]. The major difference between UDI and DA is that UDI has the upper threshold to limit very high daylight illuminance. Thus, UDI represents the operating hours during which daylight illuminance falls within a "useful" range [41,47]. A recent publication [49] further subdivided the range into three bins: from zero to 100 lux is a "non-sufficient" UDI; from 100 to 300 lux is a "supplementary" (or UDI-s) group; and from 300 to 3,000 lux is an "autonomous" (or UDI-a) group, Equation (2).

$$\text{UDI-a} = \frac{\sum_{i=1}^{N_t}(wf_i \cdot t_i)}{\sum_{i=1}^{N_t}(t_i)} \in [0,1] \text{ with}$$

$$wf_i = \begin{cases} 1 & \text{if } 300 \text{ lux} \leq I_{avail} \leq 3{,}000 \text{ lux} \\ 0 & \text{if } I_{avail} < 300 \text{ lux} \vee I_{avail} > 3{,}000 \text{ lux} \end{cases} \quad (2)$$

There are many debates on which daylight and visual comfort metrics should be used to assess daylight performance of a building [42,43,50]. In this study, we first compared UDI and LM-83-12's metrics (sDA and $ASE_{1,000/250h}$) in a spatial visualization, and later we used UDI for its temporal visualization of luminous autonomy. As UDI captures both minimum and maximum thresholds within a single metric, it can easily be incorporated into early design phases.

3.2 Thermal autonomy

There are two main thermal comfort models to derive metrics that support thermal autonomy's minimum and maximum thresholds: the adaptive model [51,52] and the Predicted Mean Vote (PMV) model [53]. In this paper, we used the ANSI/ASHRAE Standard 55's adaptive thermal comfort model to define thermal autonomy, as our basic objective is to analyze a naturally conditioned (i.e., free running) building [54]. The adaptive comfort model provides acceptable indoor operative temperature ranges based on prevailing mean outdoor temperature. Adapting the calculation method above, thermal autonomy (TA) can be calculated as:

$$TA = \frac{\sum_{i=1}^{N_t}(wf_i \cdot t_i)}{\sum_{i=1}^{N_t}(t_i)} \in [0,1]$$

$$\text{with } wf_i = \begin{cases} 0 \; if & T_{op} > 21.3\,^{\circ}\text{C} + 0.31\,T_{out} \\ 1 \; if & 14.3\,^{\circ}\text{C} + 0.31\,T_{out} \le T_{op} \le 21.3\,^{\circ}\text{C} + 0.31\,T_{out} \\ 0 \; if & T_{op} < 14.3\,^{\circ}\text{C} + 0.31\,T_{out} \end{cases} \quad (3)$$

where T_{out} is the prevailing mean outdoor air temperature (also sometimes called the running mean). It is based on a simple arithmetic mean of all of the mean daily outdoor air temperatures of all sequential days (no fewer than seven and no more than 30 days) and T_{op} is indoor operative temperature.

The adaptive comfort model includes two options for the comfort zone boundaries based on percent acceptability. We chose 80% thermal acceptability limits (for typical applications), but the 90% range could also be used. ASHRAE-55 specifies occupants' metabolic rates (1.0 to 1.3 met), their clothing (0.5 to 1.0 clo), and the prevailing mean outdoor temperature (10 to 33.5 ℃).

Thermal autonomy analysis also considers the transmitted short-wave solar radiation that falls directly onto an occupant using the SolarCal method [54,55]. It adds the effect of direct solar radiation to the Mean Radiant Temperature (MRT) values in thermal autonomy calculations.

3.3 Ventilation autonomy

ANSI/ASHRAE Standard 62.1 requires mechanical ventilation of non-residential buildings to provide indoor air quality that is acceptable to occupants and minimizes adverse health effects [56]. It specifies the minimum outdoor airflow required per zone per person, Q_{bz} determined by the Equation (5) below:

$$Q_{bz} = R_p P_z + R_a A_z \quad (5)$$

where R_p is the required outdoor airflow rate per person, P_z is the largest (peak) number of people expected to occupy the ventilation zone during typical usage, R_a is the required outdoor airflow rate per unit area, $and\ A_z$ is the net occupiable floor area of the zone. In SI units, Q_{bz} (m^3/s) can be converted into air change rate per hour (ACH) by Equation (6):

$$ACH_{req} = 3600\, Q_{bz} / V \quad (6)$$

where ACH_{req} is the minimum ACH and V (m^3) is the volume of the zone.

In this paper, we define Ventilation Autonomy (VA) as the percentage of occupied hours per year where a minimum ventilation rate can be achieved by natural ventilation only. For

calculations, we convert the minimum ventilation rate and available airflow rate into ACH units and define the VA metric as:

$$VA = \frac{\sum_{i=1}^{N_t}(wf_i \cdot t_i)}{\sum_{i=1}^{N_t}(t_i)} \in [0,1] \text{ with } wf_i = \begin{cases} 1 \text{ if } ACH_{avail} \geq ACH_{req} \\ 0 \text{ if } ACH_{avail} < ACH_{req} \end{cases} \quad (7)$$

where, t_i represents the number of occupied hours, N_t is the number of time steps, wf_i is a weighting factor depending on the ventilation thresholds, and ACH_{avail} is the available air change per hour provided by natural ventilation.

While the minimum outdoor airflow rate is the metric required by ASHRAE 62.1, carbon dioxide (CO_2) concentration in the zone could also be used as an indication of airflow rate. Therefore, CO_2 concentration can be an alternative metric for ventilation autonomy if the only source of CO_2 are people in the space and there is no gaseous air cleaner. The CO_2 limit can be calculated using Appendix D of ANSI/ASHRAE 62.1. Typical values are between 800 ppm to 1,200 ppm [57,58]. Assuming the outdoor CO_2 level as 400 ppm, we set the CO_2 thresholds of ventilation autonomy to 1,000 ppm. A different threshold could be used. Based on CO_2 concentrations, we define alternative VA metrics as:

$$VA = \frac{\sum_{i=1}^{N_t}(wf_i \cdot t_i)}{\sum_{i=1}^{N_t}(t_i)} \in [0,1] \text{ with } wf_i = \begin{cases} 1 \text{ if } \mathrm{CO}_{2,level} \geq \mathrm{CO}_{2,limit} \\ 0 \text{ if } \mathrm{CO}_{2,level} < \mathrm{CO}_{2,limit} \end{cases} \quad (8)$$

While both luminous and thermal autonomy analysis have spatial and temporal aspects, we include only temporal analysis for ventilation autonomy. In theory, ventilation autonomy could have a spatial aspect considering the possibility of non-homogeneous pollutant distribution. For simplicity, we assume that the zone is fully mixed.

4. Simulation approaches

In order to show how the multiple environmental metrics work together, we used a simplified model for simultaneous analysis with the proposed visualizations. The input parameters of the model are based on the Medium Office model of the Commercial Reference Buildings provided by the United States Department of Energy [59]. The values are representative of buildings in each climate for our proof-of-concept study; the input parameters in the simulations are not particularly important given that the purpose of this study is to show how these metrics and visualizations work together. The model (shown in Figure 2) is 5.3 x 16.0 x 2.7 m with fully-passive heating and cooling, a typical floor (single zone), and 0.48 window-to-wall ratio (0.9 m-sill height openings on the south and the north facade. The boundary conditions of the ceiling, the floor, and the east and the west facades were kept “adiabatic” to better represent the model as a single zone within a larger floor plan, with other floors above and below. The geographic locations were Phoenix, AZ (Köppen Classification: Bwh, Tropical and Subtropical Desert Climate), and Helena, MT (Köppen Classification: Dfb, Warm Summer Continental Climate), which represent hot/cold and dry climates in the US, respectively.

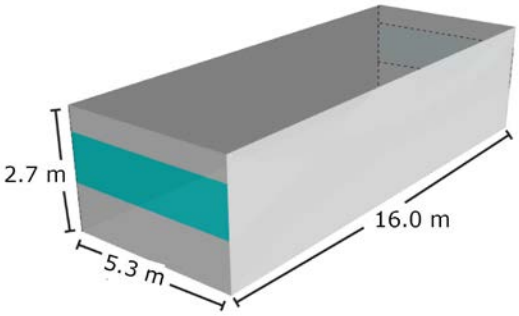

Figure 2: *A simplified model*

The applied envelope characteristics depend on the climates, as shown in Table 1. We modified visible transmittance values of window based on the other glass properties (i.e., SHGC and U-Factor) due to the limited availability in the DOE reference building inputs. We accounted for the heat gain from people; the assumption is 0.05 person/m^2 (default occupant density of office space) for peak occupancy [56] and the hourly rates differ based on the occupancy schedule of the DOE reference building and the hourly rates differ based on the occupancy schedule of the DOE reference building.

Table 1*: Envelope properties*

Climate	Location	Phoenix, AZ	Helena, MT
	Climate Zone	2B – Hot and Dry	6B – Cold and Dry
Opaque Wall	U-Factor (W/m²·K)	0.70	0.48
Window	U-Factor (W/m²·K)	5.84	3.24
	Solar Heat Gain Coefficient	0.25	0.39
	Visible Transmittance	0.55	0.55

The following sections summarize the tools and the calculation methods that we used. The users can choose any tools to simulate the hourly IEQ of the space, and the hourly simulation data can easily be converted into the proposed metrics and visualization methods.

4.1 Luminous autonomy calculations

4.1 Luminous autonomy calculations

Software: We used DIVA 4.0 and DAYSIM's annual climate-based calculations [60,61], using Radiance as the simulation engine [62].

Calculations: The analysis grid was based on a 0.6 m × 0.6 m area that was 0.8 m above the floor. We assumed the surface reflectance values as follows: 20% floor, 50% walls, 70% ceiling, 50% furniture, and 10% outside ground.

sDA calculation counts which nodes met the threshold for at least 50% of the occupied hours, and reports this as the percentage of nodes across the analysis area. It includes the effect of window shades based on the lighting standard LM-83-12 [8]. We used the conceptual DAYSIM methodology for the shade properties (0% direct transmittance and 25% diffuse transmittance). The $ASE_{1,000/250h}$ metric calculates the percentage of sensor nodes in the analysis area that are exposed to more than 1,000 lux of direct sunlight for more than 250 hours per year. UDI is the

percentage of occupied hours where the illuminance level falls within certain ranges, 300 to 3,000 lux for autonomous hours.

In this study, the daylight conditions were based on data for a typical meteorological year (TMY3), with an analysis period from 8am to 6pm local clock time (3,650 hours), accounting for daylight savings time [8]. All daylight simulations were based on ambient bounces of six and ambient division of 1,000, except ASE. ASE calculation is based on ambient bounces of zero and ambient division of 1,000 as required by LM-83-12 [8].

4.2 Thermal autonomy calculations

Software: We used Grasshopper's Honeybee to simulate spatial thermal autonomy, using EnergyPlus (v8.4) as the simulation engine [9,63,64].

Calculations: We simulated a single mean indoor air temperature for the zone and calculated the spatial distribution of thermal comfort based on the differences in MRT. MRT for each node was based on view vectors (290 evenly spaced, based on a Tregenza skydome [9]) between the node and each of the visible surfaces. The MRT calculation also implemented the SolarCal method [54,55], to assess the thermal comfort impacts of transmitted short-wave solar radiation falling directly onto an occupant. Based on the MRT values and the single-zone average air temperature, we calculated the operative temperature for each node.

Window operation was set based solely on thermal comfort requirements and was kept relatively simple for this proof-of-concept study. The minimum indoor operative temperature for natural ventilation was set to 18 ºC (the lower limit of the adaptive comfort model), and the maximum outdoor temperature was set to 28 ºC (a value considering the upper limit of the adaptive comfort model and the short-wave solar radiation effect). In practice, the window operation may be based on the more detailed settings (e.g., running mean outdoor temperature, the indoor-outdoor temperature difference, setback temperature settings, etc.) for project-specific conditions. In this paper, we chose to use generic assumptions as the major objective of the paper is showing the simultaneous workflow for integrated design. We calculated natural ventilation potential for the two windows on the south and north façades; each window opened horizontally (50% of the total window area) creating two equal-sized openings. It should be noted that preliminary analysis showed that, for the building type and climates studied, varying window area did not show significant differences compared to changing the pattern of window operation (i.e., time open/closed), so we ran our proof-of-concept simulations with a single window area openness as 50%. Climate conditions were based on data from a typical meteorological year (TMY3), with an analysis period in line with the DOE commercial reference for Medium Office model (5,270 hours).

4.3 Ventilation autonomy calculations

Software: We used EnergyPlus models to assess natural ventilation potential by simulating external and internal wind flows using Grasshopper's Honeybee [9,63,64] as the interface. We assumed well-mixed air in our analysis zone and then used bulk airflow to evaluate our natural ventilation potential. We used EnergyPlus' passive scalar transport method to calculate CO_2 concentrations as an alternative air quality indicator [65].

Calculations: In this study, we modeled only the wind effect as our proof-of-concept study model has only a single-story height and two windows on the south and north façade (we assumed that cross ventilation is the major source of natural ventilation for the model). First, we calculated the available air change per hour (ACH_{avail}) to determine how much of the required ventilation rate was provided by natural ventilation. Then, we calculated ventilation autonomy as the percentage of occupied hours per year that ACH_{avail} meets or exceeds ACH_{req}. An alternative ventilation

autonomy metric was based on CO_2 concentration rate, and we calculated the change in zone air CO_2 concentrations based on the transient air mass balance equation in EnergyPlus [65]. We used 400 ppm for the outdoor CO_2 level.

5. Results

5.1. Spatial analysis of luminous and thermal autonomy

Figure 3 shows the simulation results in a spatial format (plan view), providing a comparison between the buildings in Helena (top row) and Phoenix (bottom row). Each figure represents the different metrics present (Figures 3-A, D: UDI-a; Figures 3-B, E: ASE; Figures 3-C, F: TA). The UDI-a results (Figures 3-A and 3-D) represent the percentage of occupied hours that met both daylight sufficiency and visual comfort requirements (300 lux < illuminance < 3,000 lux), ranging from orange (100%) to blue (0%). The ASE calculations (Figures 3-B and 3-E) indicate potential glare based on the threshold of more than 1,000 lux with no ambient bounce; the grayscale pixels represent the goal of a maximum of 250 occupied hours below threshold (1,000 lux), and the pink pixels indicate the area where the nodes exceeded the threshold and therefore carry a potential for glare. Figures 3-C and 3-F (thermal autonomy) show the percentage of occupied time over one year where a sensor node met the adaptive comfort model criteria through passive means only. Note that we intentionally used number or percent of hours based on how the associated metric was defined. Designers could certainly choose to change either of these if they preferred them to be consistent.

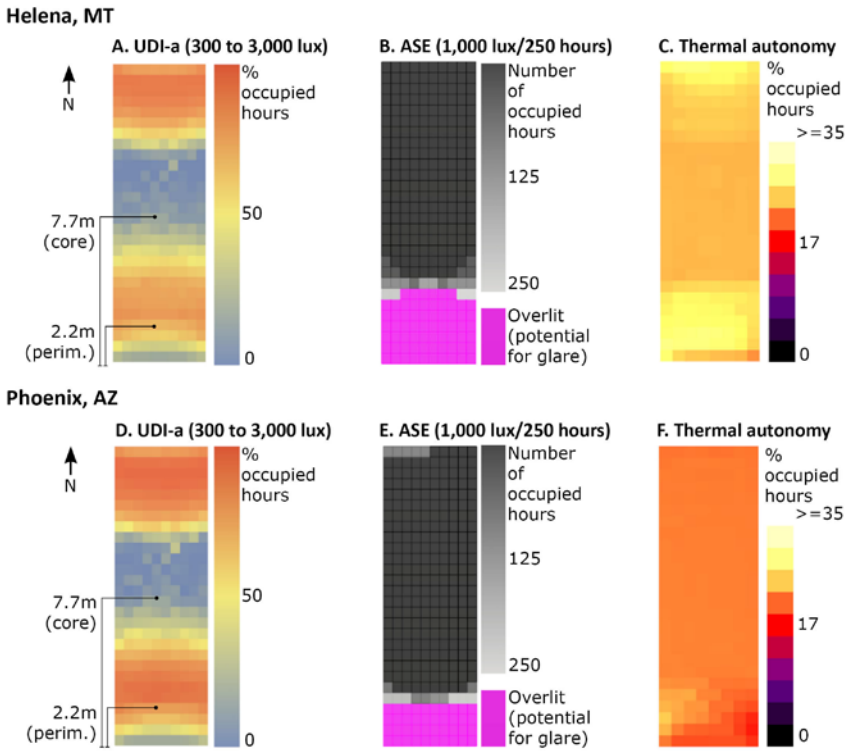

Figure 3: *Plan view comparisons between simulations of luminous autonomy (UDI-a, A. and D.; $ASE_{1000/250h}$, B. and E.) and thermal autonomy (C. and F.) in Helena, MT and Phoenix, AZ*

The results reveal that the UDI-a values in both climates have similar spatial patterns, but the Phoenix model (Figure 3-D) shows more occupied hours of luminous autonomy (i.e., more

pixels are in orange) than the Helena model (Figure 3-A). In contrast, the ASE results in Helena (Figure 3-B) demonstrate more areas with potential glare (shown in pink) than those in Phoenix (Figure 3-E). This indicates that the Helena model has less daylight sufficiency with a larger area of potential glare. This finding may be due to the fact that Helena's higher latitude leads to lower angles of the direct sun, which can penetrate deeper into the floor plan.

Regarding thermal autonomy in the colder climate of Helena (Figure 3-C), the south-facing perimeter spends a greater percentage of occupied hours within the comfort zone (shown in bright yellow) compared to the core (shown in yellow-orange). This indicates the benefit of passive solar heating during winter. In the warmer climate of Phoenix (Figure 3-F), the west side of the floor plan, closer to the south-facing window (shown in yellow), has better thermal autonomy than the east side (shown in red). This is due to the increased activity of passive solar heating in the morning (i.e., when the building has already cooled down overnight and needs some heat to reach desired temperatures) and the self-shading effect in the afternoon (i.e., when the building has been overly warmed up).

As previously noted, a clear benefit of this method is to facilitate a comparison between these different performance dimensions. When comparing the results for luminous and thermal autonomy in this example, the trade-off relationship between visual comfort and thermal comfort becomes clear. The ASE results in Helena (Figure 3-B) reveal more areas exceeding the threshold of 1,000 lux (shown in pink), indicating potential visual discomfort compared Phoenix (Figure 3-E). Although this may be counterintuitive, the higher latitude of Helena leads to a higher percentage of occupied hours with low sun angles, which is what the metric is effectively measuring (this points to some of the controversies around whether this metric is a good proxy for glare, but trying to solve that is beyond the scope of this paper). Conversely, the thermal autonomy results in Helena (Figure 3-C) indicate a higher percentage of occupied hours meeting thermal comfort requirements (shown in bright yellow), due to the potential benefit of direct sunlight for passive solar heating. This demonstrates the importance of simultaneous analysis of both luminous and thermal autonomy. To illustrate, if designers consider only the daylight results, they will simply try to make additional design decisions that decrease the area (shown in pink) of visual discomfort (i.e., increase luminous autonomy); however, doing so may have a negative impact on thermal autonomy when passive solar heating is taken into consideration. The Appendix includes the summary table of Figure 3 and further discussion regarding the results.

The spatial maps (Figure 3) represent annual values but it may not be enough for a designer to understand the times of the year that a building requires solar control (e.g., deploying shades) or natural ventilation (e.g., operable windows) to mitigate both luminous and thermal discomfort. In the following sections, we propose a method for the simultaneous analysis of luminous and thermal metrics via temporal visualizations.

5.2. Temporal analysis of luminous, thermal, and ventilation autonomy

Although the concepts of luminous and thermal autonomy are similar, some aspects of their calculations differ. For example, in our simulations, the initial calculations (Figure 3) were based on the different periods of analysis. To allow for comparisons between the luminous and thermal metrics while using the same format, the simulated data had to be pre- and post-processed. This includes adjusting the period of analysis (which meets both the lighting standard, LM-83-12, and the DOE commercial reference building occupancy schedules, equaling a total of 3,130 occupied hours); creating an annual heat map for a specific point in the analytical grid; and generating data visualizations to show when the hours of luminous, thermal, and ventilation autonomy occur over one year. As an example, the following subsections present the temporal data of a building in

Phoenix collected from a point on the floor plan (2.2 m from the façade), which represents the perimeter zone (for reference, see Figure 3-D). We first show the temporal visualization for ventilation autonomy (Section 5.2.1), which is a new metric, then we add it into the visualizations for all three metrics of environmental autonomy (Section 5.2.2).

5.2.1 Temporal visualization for ventilation autonomy

Figure 4 represents the hourly and yearly ventilation autonomy of the building in Phoenix (a similar visualization could be made for the Helena location, but it is not reported here for the sake of brevity). In this section, we visualize the ventilation autonomy based both on outdoor airflow rate and CO_2 concentration (given that ventilation autonomy is a new concept, we are explicitly using both approaches from ANSI/ASHRAE Standard 62.1). The color legend represents whether the respective parameters meet the minimum thresholds for ventilation rate (Figures 4-A and 4-B) and CO_2 concentration (Figures 4-C and 4-D): black for the hours that did not meet minimum thresholds and yellow for the hours that met or exceeded them. The leftmost images (Figures 4-A and 4-C) display the hourly ventilation autonomy data as an annual heat map. The x-axis represents the months of the year (January 1–December 31), and the y-axis represents the hours in a day. The white area refers to unoccupied hours, which were excluded from the analysis. In the right side images (Figures 4-B and 4-D), the annual summary graphs are displayed, which shows the percentages of occupied hours with ventilation autonomy. These figures provide a summary of the conditions outside the comfort range and helps quantify the effects of parametric changes within the building.

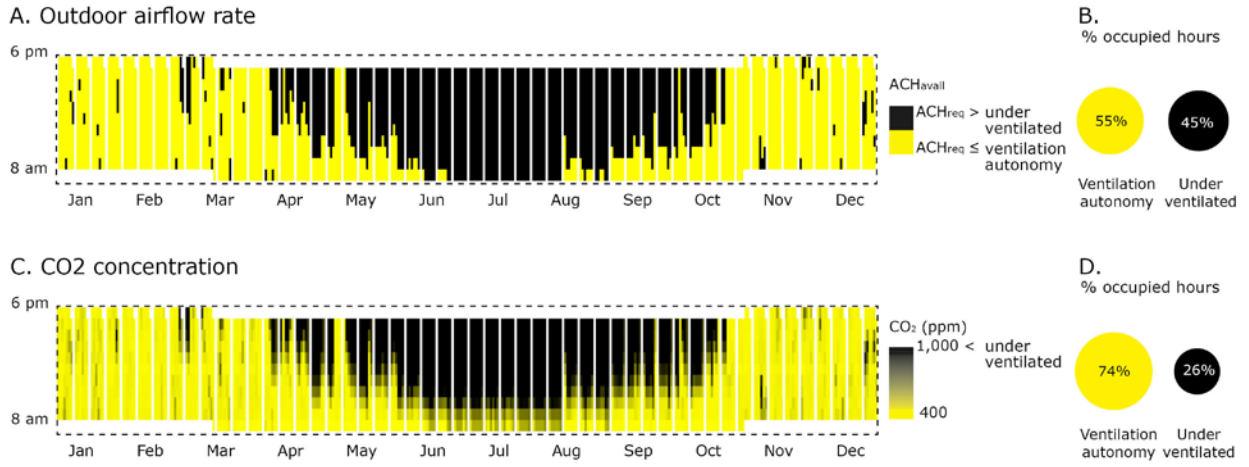

Figure 4: *Hourly map of ventilation autonomy and annual summary for Phoenix, AZ*

As shown in Figures 4-A and 4-B, 55% of the occupied hours of the Phoenix building meet the minimum outdoor airflow rate required by ASHRAE 62.1 [56]. The hours that do not meet the outdoor airflow rate could be due to the windows being closed because of the window opening criteria we used, indoor/outdoor temperature ranges, or insufficient cross ventilation resulting from wind speed or direction. Regarding the CO_2 concentration metric (Figures 4-C and 4-D), 74% of the occupied hours meet the minimum requirement of 1,000 ppm. The differences between Figures 4-A and 4-C are due to the fact that ASHRAE 62.1 requires peak occupancy design conditions for minimum outdoor airflow rate, while CO_2 concentration varies according to the typical occupancy rates. Designers and engineers can choose either metric to represent the ventilation autonomy of a building.

5.2.2 Temporal visualizations for luminous, thermal, and ventilation autonomy

Figure 5 is the legend that will be used for subsequent graphs, and shows the color scheme representing the periods of visual, thermal, and ventilation comfort, including:
Left image:

- overly warm (shown in red; occupied hours exceeding the upper limit of the adaptive thermal-comfort criteria),
- overly cool (shown in blue; occupied hours exceeding the lower limit of the adaptive thermal-comfort criteria),
- underlit (shown in dark yellow/green; low illuminance: < 300 lux; UDI: lower thresholds),
- overlit (shown in pale yellow; potential glare: > 3,000 lux; UDI: upper thresholds),
- Note that the middle horizontal row all represents thermal autonomy, while the middle vertical column all represents luminous autonomy, with the yellow circle in the middle representing that both are occurring simultaneously

Right image:

- under-ventilated (shown in black; high CO_2 concentration: > 1,000 ppm), and
- ventilation autonomy (shown in yellow).

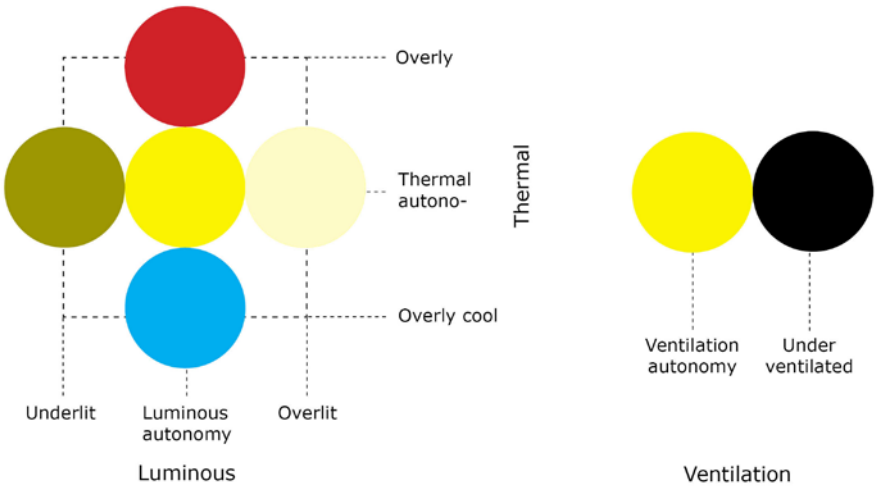

Figure 5: *Proposed color scheme*

In Figure 6, the size of each bubble represents the extent of each period (i.e., the percentage of occupied hours that fall within or outside of each category of autonomy) to show the summary of the annual data. Using that color scheme, Figure 6 shows parallel visualizations for luminous (A), thermal (B), and ventilation autonomy (C) in the building in Phoenix, AZ.

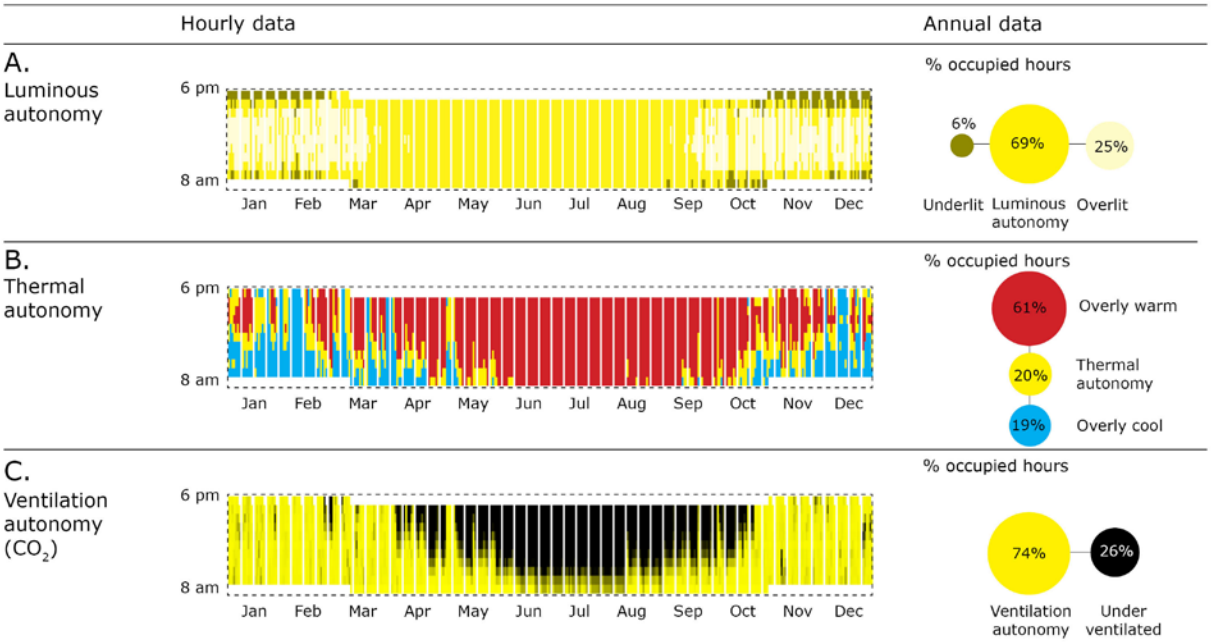

Figure 6: *Hourly autonomy map and annual summary – Phoenix, AZ*

5.3 Simultaneous analysis of luminous and thermal autonomy

5.3.1 Hourly data visualizations

This paper proposes the integration of hourly data visualizations into the simultaneous analysis of luminous and thermal autonomy. As shown in Figure 7, we expanded the legend shown in Figure 5 to now include the corners and defined nine colors for describing the simultaneous luminous and thermal conditions and whether they fell within or outside of the limits of autonomy.

Figure 7: *Nine colors representing the luminous and thermal characteristics of a building*

By applying the color scheme to the hourly visualizations (Figure 8), we demonstrate the usefulness of plotting hourly results simultaneously for both thermal and luminous autonomy. These visualizations will allow designers and engineers to better understand when luminous and thermal autonomy occurs throughout the year, along with each combination of these two metrics.

Figure 8 compares the luminous and thermal autonomy between the buildings in Phoenix and Helena using the combined color scheme. The figures on the left (8-A, 8-C, 8-E, 8-G) display the hourly data as annual heat maps, while the figures on the right (8-B, 8-D, 8-F, 8-H) represent the annual summary graphs (i.e., percentages of occupied hours in each state of environmental autonomy) measured at a specific point in each test climate. The dark blue (overly cool and underlit) areas indicate opportunities for increased passive solar heating, while the light blue (overly cool and overlit) areas indicate a need for passive solar heating that is implemented more carefully to avoid potential glare. For example, in Helena (8-A), 19% of the occupied hours are overlit, but the thermal conditions are either autonomous or overly cool for most of the time.

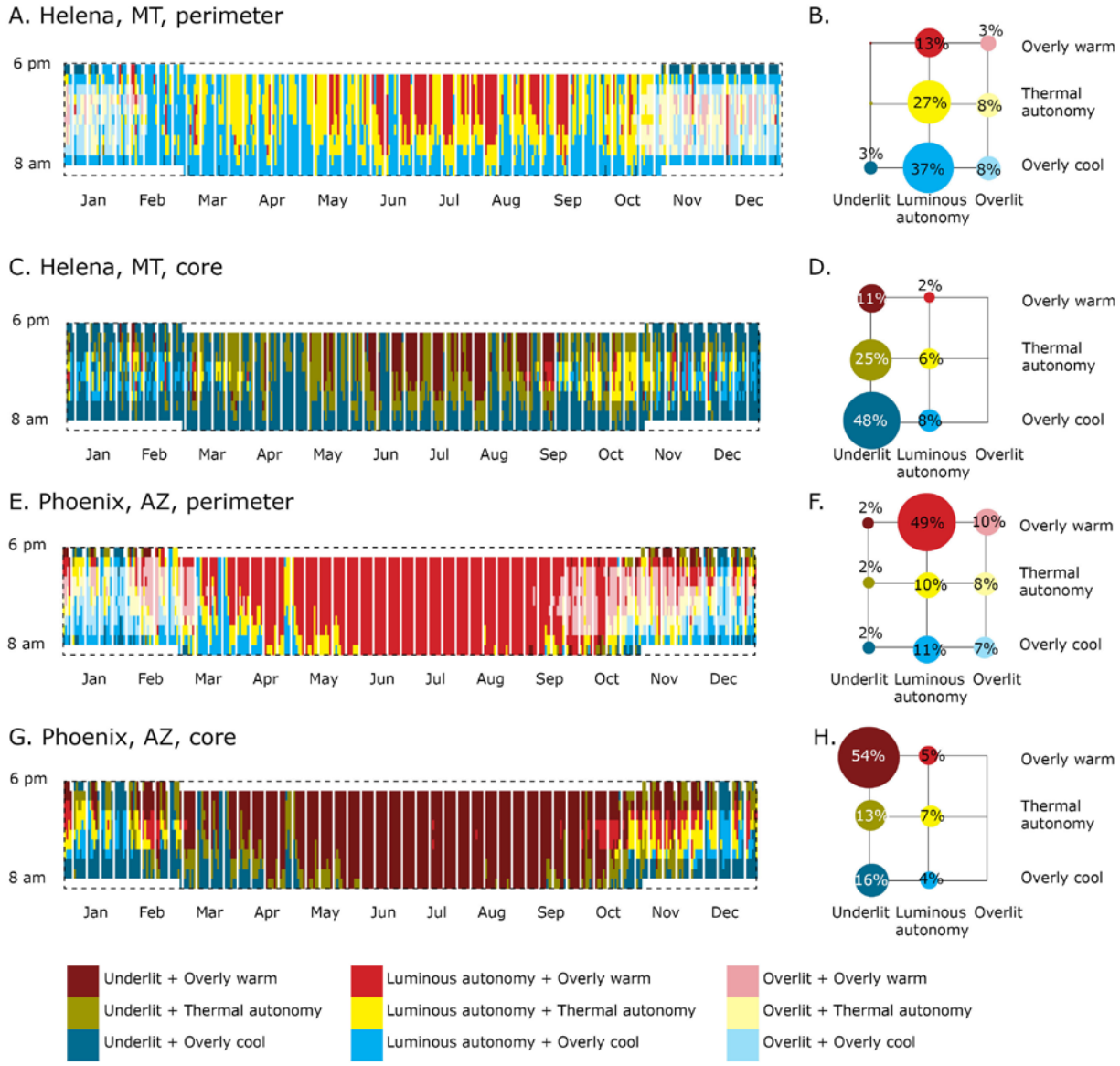

Figure 8: *Simultaneous analysis of luminous and thermal autonomy: hourly autonomy map and annual summary; A. and B.: Helena, south-facing perimeter; C. and D.: Helena, core; E. and F.: Phoenix, south-facing perimeter; G. and H.: Phoenix, core.*

These percentages occur from October through March, which indicates that during overlit hours (in which shades are pulled down to block the sunlight), shading may exacerbate the overly cool

state of the building, as they cause a reduction in passive solar heating in the morning. The pink (overly warm and overlit) areas most likely occur when the building is warmed by the direct sun; this is, when shades are needed. The dark red (overly warm and underlit) areas occur late in the afternoon, when there is less sunlight but too much thermal energy; during these times, the building needs supplemental lighting and cooling, ideally through passive means.

5.3.2 Application: Internal shade simulations

Internal fabric shade is a common strategy for solar-radiation control that has a simultaneous impact on thermal and luminous autonomy. We tested two types of fabric shades and two control strategies (Table 2) to demonstrate the impact of internal shade on both thermal and luminous autonomy. The thermal properties of the fabric shade were set as emissivity = 0.75, and thermal conductivity = 0.17 W/m·K, which are typical values for polyester fabric. Regarding shade controls, we tested the LM-83 sDA manual shade control and an idealistic dynamic control using a horizontal illuminance threshold of 3,000 lux.

***Table 2**: Internal shade types and control strategies*

	Description
Shade type	0% direct and 5% diffused visual-light transmission, the IES LM-83 recommendations.
	0% direct and 25% diffused visual-light transmission, the DAYSIM default fabric shade value.
Shade control	Shade is deployed when 2% of floor area receives direct sunlight (representing a manual control), the IES LM-83 requirements.
	Shade is deployed when a sensor (located 0.6 m from the façade at the desk) receives more than 3,000 lux, representing an automated control.

We tested several combinations of these two variables in the following experiments:

- low-transmittance shade + automated control,
- low-transmittance shade + manual control,
- high-transmittance shade + manual control

The manual control demonstrated a higher frequency (more hours) of shade deployment compared to the automated control.

Figure 9 summarizes the relative impacts of the selected shade types and their controls on the annual hours of thermal and luminous autonomy in the Phoenix building. When comparing the results, the “low-transmittance shade + automated control” experiment performed the best (i.e., this setting achieved the maximum hours of autonomy). The default setting of LM-83-12, represented by “low-transmittance shade + manual control,” tends to be more stringent (frequent shade deployment), as it created a greater number of underlit hours than the other combinations. Although the “high transmittance shade + manual control” experiment performed better than the “low transmittance shade + manual control” experiment, 4% of the occupied hours were overlit. We can thus conclude that it is best to have less frequent shade deployments and use low-transmittance fabric type in Phoenix.

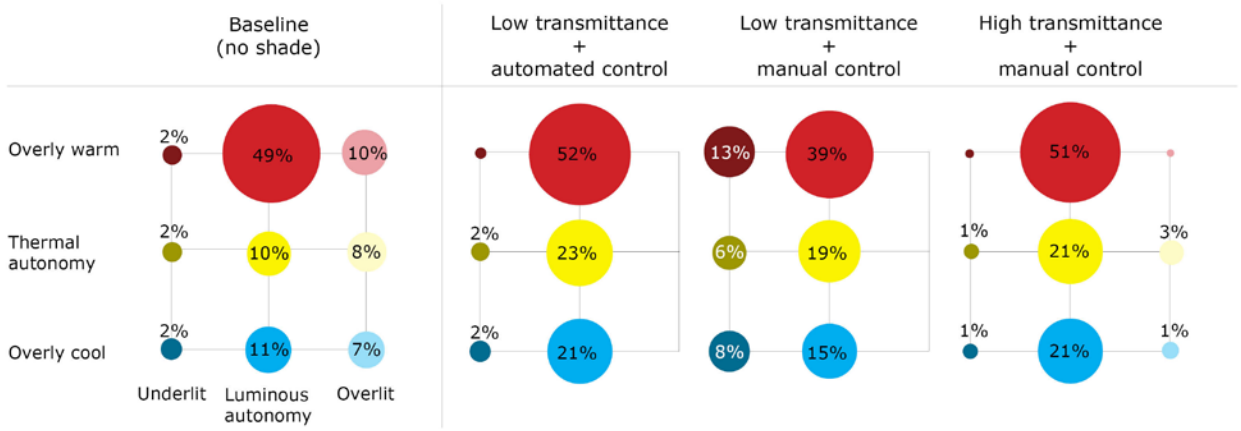

Figure 9: *The impacts of internal shades on annual hours of luminous and thermal autonomy in the building in Phoenix, AZ*

These results reveal the interesting design challenges that can emerge from examining the simultaneous analysis of thermal and visual autonomy, indicating that designers should evaluate the impact of internal shades in the early design phase while considering the control strategies and fabric properties that are most suitable for the target climate. Designers can also use simultaneous analysis for other design elements that can impact the luminous and thermal aspects of a building, such as external shades.

5.4 Simultaneous analysis of thermal and ventilation autonomy

5.4.1 Hourly data visualizations

This paper also proposes the integration of hourly data visualizations into the simultaneous analysis of thermal and ventilation autonomy. As shown in the legend illustrated in Figure 10, we defined six combinations of color and line patterns for describing the simultaneous conditions of thermal and ventilation autonomy.

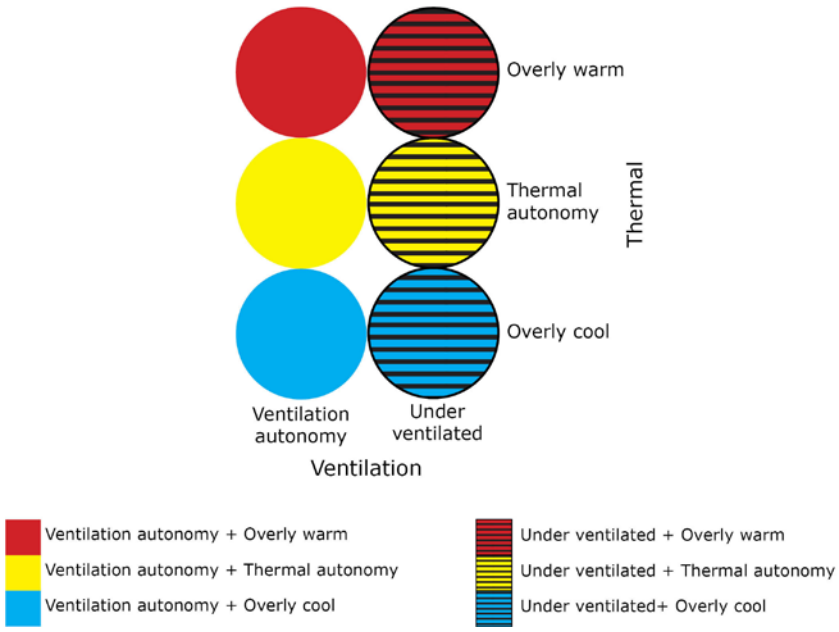

Figure 10: *Six combinations of color and line patterns representing the thermal and ventilation characteristics of a building*

These visualizations will allow designers and engineers to better understand when thermal and ventilation autonomy occurs throughout the year, along with each combination of these two metrics.

Figure 11 provides an example of the simultaneous analysis of thermal and ventilation autonomy within the Phoenix building, using both an hourly map and an annual graph. The data shows that most of the summer hours are overly warm and under ventilated; in contrast, any periods that show either thermal autonomy or are overly cool are receiving adequate ventilation. In the following section (5.4.2), we will try to maximize ventilation autonomy by introducing a partial window opening when the building is under ventilated while ensuring minimal thermal impact.

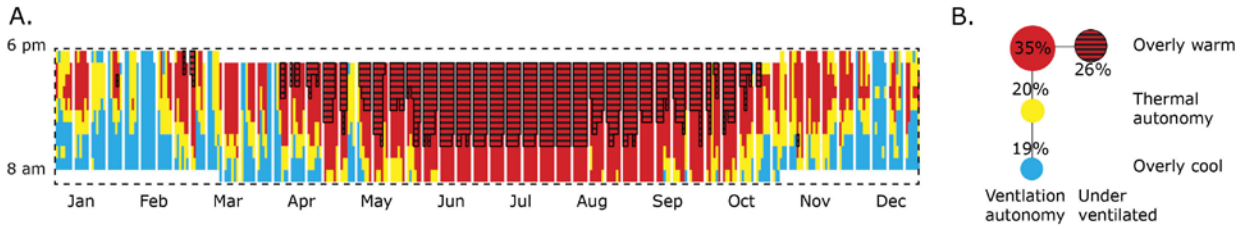

Figure 11: *Simultaneous analysis of thermal and ventilation autonomy in a building in Phoenix, AZ; A. Hourly autonomy map; B. Annual autonomy summary*

5.4.2 Application: A partial window opening

Operable windows are a common strategy for the natural cooling and ventilation of buildings. When opening a window, there is a simultaneous impact on thermal and ventilation autonomy. Using the simulation of a building in Phoenix, we tested the effect of opening the windows just partially outside of window-operation hours (i.e., the hours that the windows are open otherwise closed to avoid over-heating/cooling); the goal was to determine whether we can increase the number of hours that meet minimum ventilation requirements while minimizing the impact on thermal autonomy. A partial window opening or a trickle vent built into the façade can be introduced when there is insufficient ventilation, thereby allowing a small amount of air movement between the interior and exterior. By testing different fractions of opening areas, we compared the relative impacts of operable windows on both ventilation and thermal autonomy.

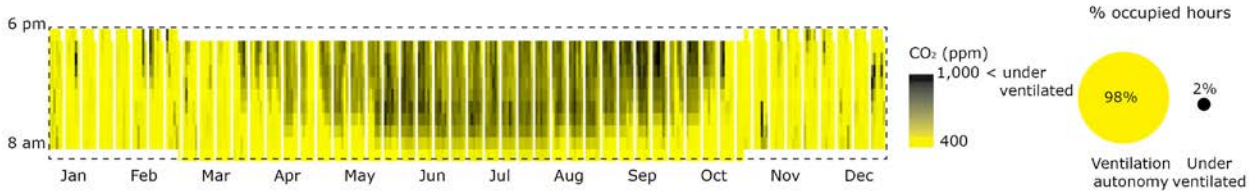

Figure 12: *Hourly map of ventilation autonomy and annual summary graph based on CO_2 concentration in a building in Phoenix, AZ; A. and B.: 2.5% opening outside of normal window-operation hours*

Figure 12 illustrates the temporal change in the relative impact of a partial window opening (2.5% of the total window area) on ventilation autonomy. The partial opening helped increase the percentage of occupied hours that met the minimum air change rate, from 74% (Figure 4-D; baseline) to 98% (Figure 12-B; 2.5% opening). This indicates that just a small opening, such as 2.5% of the operable window area, is sufficient for achieving ventilation autonomy. Now checking for the effect of this partial window opening on thermal performance, the impacts were relatively

negligible (i.e., the partial opening did not change the thermal conditions, which remain overly warm in Phoenix). Regarding operative temperature, the partial opening did not have much of an effect (the changes were less than 1°C). We can thus conclude that the application of a partial window opening outside of normal window-operation hours may be beneficial in Phoenix, as it increases the occupied hours of ventilation autonomy while keeping the thermal impact low. This experiment demonstrates the usefulness of a simultaneous analysis of ventilation and thermal autonomy in helping designers understand the relative impacts of operable windows and the areas in which they would be most effective.

6. Discussion

Throughout each subsection in section 5, the proposed workflow and visualization methods have shown the potential of the temporal visualizations for simultaneous analysis of ventilation, thermal, and luminous autonomy.

Categorizing the thermal and visual characteristics into nine combinations is useful, as each combination can guide different design and analysis considerations. At first glance, designers can try to maximize the hours meeting both thermal and luminous thresholds (represented in yellow). However, the further contribution of the visualization methods is that it allows designers to consider multiple environmental effects in the early phase of building design. For example, when a building is overly cool and overlit, designers should carefully analyze the potential benefits of passive solar heating (and how to achieve this without introducing glare) versus the negative effects of reducing solar load simply to resolve the issue of overlighting. In contrast, when it is overly cool and underlit, the space simply needs more heating and lighting. This typically happens either deep within the floor plan or early in the morning when the building lacks sufficient thermal energy and daylight levels for the occupants. Overly warm and overlit conditions most often occur when it is warm, and there is direct sun; this is when the building needs shades or blinds. Overly warm and underlit conditions occur late in the afternoon when there is less sunlight but too much thermal energy; during these times, the building needs supplemental lighting and cooling.

The temporal analysis of ventilation autonomy, which is for the first time defined and introduced in this paper, shows the minimum required design consideration for indoor air quality through the building envelope (currently, the majority of the sealed building do not have the requirements). The consideration is important as indoor air quality has a stronger health impact on people than thermal comfort, and arguably, more than lighting [66–68]. The proposed visualization and workflow provide an integrated approach for both architectural and mechanical/electrical designers. It shows the benefits of evaluating the simultaneous impacts of utilizing operable windows for indoor air quality on both thermal and ventilation aspects. As shown in section 5.4, applying a partial opening outside of normal window-operation hours can be useful in saving energy required to provide the proper outdoor ventilation rate, especially when there is minimal impact on thermal autonomy, such as in the case of the building in Phoenix, AZ (see section 5.4.2). This is an example of the usefulness of the proposed workflow and visualization methods. We can expand the use of ventilation autonomy further by including ventilation efficiency and spatial differences. It would help designers with building layout design which depends on the size of the perimeter zones and the micro-climate with wind access and favorable outdoor temperatures.

7. Limitations and future studies

This paper proposed a method as well as a visualization to simultaneously analyze the ventilation, thermal, and luminous characteristics of a building, and also used a very simple

building model as a proof-of-concept exercise. Notably, there are several limitations to the proposed assessment method.

For visual comfort, this study used illuminance-based metrics to analyze direct sunlight illuminance on a horizontal surface of each node. This metric is often criticized for its lack of directionality and luminance-related aspects, which are important in visual comfort predictions. The more accurate, but more challenging, luminance-based metrics (e.g., Daylight Glare Probability) can be applied to the workflow if the designers know the primary view angles of the occupants and have both the time and expertise needed to tackle the accompanying complex simulations.

The current study only explored internal shading performance regarding solar control and shade material properties; future studies should examine shading systems in more detail because they can have multiple impacts on building performance (i.e., an integrated system with light dimming that affects lighting energy load, which in turn affects internal heat gain; the evaluation of simultaneous impacts of an external shading and electrochromic glass, etc.).

For natural ventilation calculations, this study used a simplified airflow calculation method to predict the hourly air change rate based on wind-driven air movement. In a more realistic design, it would need to include the stack effect. In addition, accounting for thermal comfort implications of elevated air speeds (such as the use of a fan) and humidity would provide additional value. For the relatively dry climates we studied, humidity is not a major source of thermal discomfort. While the adaptive model in ASHRAE-55 does not take humidity into account, the original one did. For assessing other climates in the future, we would likely use the original adaptive model which used effective temperature (ET*; the operative temperature of an enclosure at 50 % relative humidity that would cause the same sensible plus latent heat exchange from a person as would the actual environment) as the outdoor climate index which includes humidity [51,69].

The use of Computational Fluid Dynamic methods would allow the designers to predict the spatial distribution of ventilation autonomy. This would be especially important when the building has a complex floorplan with multiple zones or uses stratification-based air distribution systems as displacement ventilation or underfloor air distribution.

As briefly mentioned in section 5.4, the currently defined ventilation autonomy metric is relatively simple (compared to luminous and thermal autonomy metrics). But there is potential for further development, for example by removing the assumption of homogenous air distribution or using the Indoor Air Quality procedure described in ASHRAE 62.1. In terms of practical applications, the hourly data from the simultaneous analyses may be implemented in the building automation system and localized comfort system.

An increasing number of buildings have mixed-mode systems and automated shading systems in place to achieve high performance in energy and occupant comfort. Often, these control systems lack an integration of multiple environmental aspects, thereby making some occupants uncomfortable and distracted, especially in the perimeter zone. The multi-autonomy workflow can help in the selection of the proper shade/window types and control systems that will respond to the diurnal and seasonal variations in the visual, thermal, and air quality comfort of a building.

Introducing optimization algorithms to inform early design decision making could be another next step that might benefit from using multiple autonomy metrics. The proposed autonomy framework could enhance existing optimization processes by bringing the three environmental aspects into a single workflow. The optimization process can support the designers by selecting a better building envelope design or operation methods by illustrating the trade-offs when trying to maximize autonomy hours for ventilation, thermal, and luminous aspects.

8. Conclusions

In this paper, we simultaneously assessed ventilation, thermal and luminous autonomy with a new method of visualizing the hourly comfort data. The visualizations categorize thermal and visual comfort in nine combinations, allowing the designers to understand these two metrics in an hourly format. We also defined and developed a new ventilation autonomy metric that can be implemented in the overall building autonomy workflow. Using a comparative example in two climates, we learned that the conventional building analysis workflow, where luminous or thermal autonomy metrics are considered in isolation, might inherently inhibit the use of passive solar heating in higher latitude locations (i.e., the hours when it is overly cool yet overly lit). The simultaneous analysis also illustrated the potential of having small partial openings outside of standard window-operation hours to achieve ventilation autonomy while having a minimal impact in thermal autonomy. The new method for simultaneously visualizing ventilation, thermal, and lighting comfort data will help designers create more integrated designs by providing a better understanding of the trade-off relationships that occur among multiple environmental aspects. Building envelope design and control strategies can be better integrated based on the proposed workflow and visualizations.

9. Acknowledgement

This study was sponsored by Center for Built Environment (CBE) and the Republic of Singapore's National Research Foundation through a grant to the Berkeley Education Alliance for Research in Singapore (BEARS) for the Singapore-Berkeley Building Efficiency and Sustainability in the Tropics (SinBerBEST) Program.

10. References

[1] B. Vale, R. Vale, The new autonomous house: Design and planning for sustainability, Thames & Hudson London, 2000.

[2] S.-Y. Chen, C.-Y. Chu, M. Cheng, C.-Y. Lin, The Autonomous House: A Bio-Hydrogen Based Energy Self-Sufficient Approach, Int. J. Environ. Res. Public. Health. 6 (2009) 1515–1529. doi:10.3390/ijerph6041515.

[3] A.B. Smith, R.W. Katz, US billion-dollar weather and climate disasters: data sources, trends, accuracy and biases, Nat. Hazards. 67 (2013) 387–410. doi:10.1007/s11069-013-0566-5.

[4] N. Achour, A.D.F. Price, Resilience strategies of healthcare facilities: present and future, Int. J. Disaster Resil. Built Environ. 1 (2010) 264–276. doi:10.1108/17595901011080869.

[5] USGBC, LEED v4 for Building Design and Construction, Washington, DC, US, 2014. http://www.usgbc.org/resources/leed-v4-building-design-and-construction-current-version (accessed September 8, 2017).

[6] R. Phillips, L. Troup, D. Fannon, M.J. Eckelman, Do resilient and sustainable design strategies conflict in commercial buildings? A critical analysis of existing resilient building frameworks and their sustainability implications, Energy Build. 146 (2017) 295–311. doi:10.1016/j.enbuild.2017.04.009.

[7] B. Levitt, M. Ubbelohde, G. Loisos, N. Brown, Thermal autonomy as metric and design process, in: CaGBC Natl. Conf. Expo Push. Boundary–Net Posit. Build., 2013: pp. 47–58.

[8] IES, Approved Method: IES Spatial Daylight Autonomy (sDA) and Annual Sunlight Exposure (ASE), Illuminating Engineering Society of North America, New York, NY, US, 2012.

[9] C.W. Mackey, Pan climatic humans: shaping thermal habits in an unconditioned society, Master thesis, Massachusetts Institute of Technology, 2015. http://dspace.mit.edu/handle/1721.1/99261 (accessed January 5, 2018).
[10] W.G. Reed, E.B. Gordon, Integrated design and building process: what research and methodologies are needed?, Build. Res. Inf. 28 (2000) 325–337. doi:10.1080/096132100418483.
[11] M. Lewis, Integrated Design for Sustainable Buildings, ASHRAE J. N. Y. 46 (2004) S22–S26, S28–S30.
[12] A. McGregor, C. Roberts, F. Cousins, Two Degrees: The Built Environment and Our Changing Climate, 1 edition, Routledge, Abingdon, Oxon ; New York, NY, 2012.
[13] C.F. Reinhart, J. Wienold, The daylighting dashboard – A simulation-based design analysis for daylit spaces, Build. Environ. 46 (2011) 386–396. doi:10.1016/j.buildenv.2010.08.001.
[14] S. Attia, J.L.M. Hensen, L. Beltrán, A.D. Herde, Selection criteria for building performance simulation tools: contrasting architects' and engineers' needs, J. Build. Perform. Simul. 5 (2012) 155–169. doi:10.1080/19401493.2010.549573.
[15] W.L. Lee, A comprehensive review of metrics of building environmental assessment schemes, Energy Build. 62 (2013) 403–413. doi:10.1016/j.enbuild.2013.03.014.
[16] IEA, IPEEC, Building Energy Performance Metrics, 2015. https://www.iea.org/publications/freepublications/publication/BuildingEnergyPerformanceMetrics.pdf (accessed January 14, 2018).
[17] M. Andersen, Unweaving the human response in daylighting design, Build. Environ. 91 (2015) 101–117. doi:10.1016/j.buildenv.2015.03.014.
[18] J.A. Jakubiec, M.C. Doelling, O. Heckmann, R. Thambiraj, V. Jathar, Dynamic Building Environment Dashboard: Spatial Simulation Data Visualization in Sustainable Design, Technol. Des. 1 (2017) 27–40. doi:10.1080/24751448.2017.1292791.
[19] F. Sicurella, G. Evola, E. Wurtz, A statistical approach for the evaluation of thermal and visual comfort in free-running buildings, Energy Build. 47 (2012) 402–410. doi:10.1016/j.enbuild.2011.12.013.
[20] Z. Luo, J. Zhao, J. Gao, L. He, Estimating natural-ventilation potential considering both thermal comfort and IAQ issues, Build. Environ. 42 (2007) 2289–2298. doi:10.1016/j.buildenv.2006.04.024.
[21] M. David, M. Donn, F. Garde, A. Lenoir, Assessment of the thermal and visual efficiency of solar shades, Build. Environ. 46 (2011) 1489–1496. doi:10.1016/j.buildenv.2011.01.022.
[22] W.N. Hien, W. Liping, A.N. Chandra, A.R. Pandey, W. Xiaolin, Effects of double glazed facade on energy consumption, thermal comfort and condensation for a typical office building in Singapore, Energy Build. 37 (2005) 563–572. doi:10.1016/j.enbuild.2004.08.004.
[23] M.V. Nielsen, S. Svendsen, L.B. Jensen, Quantifying the potential of automated dynamic solar shading in office buildings through integrated simulations of energy and daylight, Sol. Energy. 85 (2011) 757–768. doi:10.1016/j.solener.2011.01.010.
[24] H. Shen, A. Tzempelikos, Sensitivity analysis on daylighting and energy performance of perimeter offices with automated shading, Build. Environ. 59 (2013) 303–314. doi:10.1016/j.buildenv.2012.08.028.
[25] R. Hwang, S. Shu, Building envelope regulations on thermal comfort in glass facade buildings and energy-saving potential for PMV-based comfort control, Build. Environ. 46 (2011) 824–834. doi:10.1016/j.buildenv.2010.10.009.

[26] L. Vanhoutteghem, G.C.J. Skarning, C.A. Hviid, S. Svendsen, Impact of façade window design on energy, daylighting and thermal comfort in nearly zero-energy houses, Energy Build. 102 (2015) 149–156. doi:10.1016/j.enbuild.2015.05.018.
[27] P.R. Lyons, D. Arasteh, C. Huizenga, Window performance for human thermal comfort, ASHRAE Trans. Atlanta. 106 (2000) 594.
[28] C. Huizenga, H. Zhang, P. Mattelaer, T. Yu, E.A. Arens, P. Lyons, Window performance for human thermal comfort, The national fenestration rating council, 2006.
[29] D. Rowe, Effect on Thermal Comfort of Radiant Heat Exchange Near Single Glazed Windows, Archit. Sci. Rev. 46 (2003) 29–35. doi:10.1080/00038628.2003.9696961.
[30] G. Gan, Analysis of mean radiant temperature and thermal comfort, Build. Serv. Eng. Res. Technol. Lond. 22 (2001) 95–101. doi:http://dx.doi.org.libproxy.berkeley.edu/10.1191/014362401701524154.
[31] F. Cappelletti, A. Prada, P. Romagnoni, A. Gasparella, Passive performance of glazed components in heating and cooling of an open-space office under controlled indoor thermal comfort, Build. Environ. 72 (2014) 131–144. doi:10.1016/j.buildenv.2013.10.022.
[32] C. Marino, A. Nucara, M. Pietrafesa, Mapping of the indoor comfort conditions considering the effect of solar radiation, Sol. Energy. 113 (2015) 63–77. doi:10.1016/j.solener.2014.12.020.
[33] M. Bessoudo, A. Tzempelikos, A.K. Athienitis, R. Zmeureanu, Indoor thermal environmental conditions near glazed facades with shading devices – Part I: Experiments and building thermal model, Build. Environ. 45 (2010) 2506–2516. doi:10.1016/j.buildenv.2010.05.013.
[34] M. Boubekri, I.N. Cheung, K.J. Reid, C.-H. Wang, P.C. Zee, Impact of Windows and Daylight Exposure on Overall Health and Sleep Quality of Office Workers: A Case-Control Pilot Study, J. Clin. Sleep Med. JCSM Off. Publ. Am. Acad. Sleep Med. 10 (2014) 603–611. doi:10.5664/jcsm.3780.
[35] M.B.C. Aries, J.A. Veitch, G.R. Newsham, Windows, view, and office characteristics predict physical and psychological discomfort, J. Environ. Psychol. 30 (2010) 533–541. doi:10.1016/j.jenvp.2009.12.004.
[36] K.M. Farley, J.A. Veitch, A room with a view: A review of the effects of windows on work and well-being, National Research Council Canada, 2001.
[37] P. Leather, M. Pyrgas, D. Beale, C. Lawrence, Windows in the Workplace: Sunlight, View, and Occupational Stress, Environ. Behav. 30 (1998) 739–762. doi:10.1177/001391659803000601.
[38] W. O'Brien, I. Gaetani, S. Carlucci, P.-J. Hoes, J.L.M. Hensen, On occupant-centric building performance metrics, Build. Environ. 122 (2017) 373–385. doi:10.1016/j.buildenv.2017.06.028.
[39] A.M. Atzeri, F. Cappelletti, A. Tzempelikos, A. Gasparella, Comfort metrics for an integrated evaluation of buildings performance, Energy Build. 127 (2016) 411–424. doi:10.1016/j.enbuild.2016.06.007.
[40] IES, The Lighting Handbook, 10th Edition, Illuminating Engineering Society, 2011. https://www.ies.org/store/lighting-handbooks/lighting-handbook-10th-edition/ (accessed January 17, 2018).
[41] C.F. Reinhart, J. Mardaljevic, Z. Rogers, Dynamic Daylight Performance Metrics for Sustainable Building Design, LEUKOS. 3 (2006) 7–31. doi:10.1582/LEUKOS.2006.03.01.001.

[42] K. Van Den Wymelenberg, M. Inanici, Evaluating a New Suite of Luminance-Based Design Metrics for Predicting Human Visual Comfort in Offices with Daylight, LEUKOS. 12 (2016) 113–138. doi:10.1080/15502724.2015.1062392.
[43] J. Jakubiec, C. Reinhart, The "adaptive zone" – A concept for assessing discomfort glare throughout daylit spaces, Light. Res. Technol. 44 (2012) 149–170. doi:10.1177/1477153511420097.
[44] J.Y. Suk, M. Schiler, K. Kensek, Development of new daylight glare analysis methodology using absolute glare factor and relative glare factor, Energy Build. 64 (2013) 113–122. doi:10.1016/j.enbuild.2013.04.020.
[45] S. Carlucci, F. Causone, F. De Rosa, L. Pagliano, A review of indices for assessing visual comfort with a view to their use in optimization processes to support building integrated design, Renew. Sustain. Energy Rev. 47 (2015) 1016–1033. doi:10.1016/j.rser.2015.03.062.
[46] M.G. Kent, S. Altomonte, P.R. Tregenza, R. Wilson, Temporal variables and personal factors in glare sensation, Light. Res. Technol. 48 (2016) 689–710. doi:10.1177/1477153515578310.
[47] A. Nabil, J. Mardaljevic, Useful daylight illuminance: a new paradigm for assessing daylight in buildings, Light. Res. Technol. 37 (2005) 41–57. doi:10.1191/1365782805li128oa.
[48] Education Funding Agency, EFA daylight design guide, London, UK, 2014. https://www.gov.uk/government/publications/efa-daylight-design-guide (accessed January 17, 2018).
[49] J. Mardaljevic, M. Andersen, N. Roy, J. Christoffersen, Daylighting Metrics: Is there a relation between Useful Daylight Illuminance and Daylight Glare Probabilty?, Proc. Build. Simul. Optim. Conf. BSO12. (2012). https://infoscience.epfl.ch/record/179939 (accessed September 22, 2017).
[50] F. Cantin, M-C. Dubois, Daylighting metrics based on illuminance, distribution, glare and directivity, Light. Res. Technol. 43 (2011) 291–307. doi:10.1177/1477153510393319.
[51] R.J. de Dear, G. Brager, Developing an adaptive model of thermal comfort and preference, ASHRAE Trans. 104 (1998).
[52] J.F. Nicol, M.A. Humphreys, Adaptive thermal comfort and sustainable thermal standards for buildings, Energy Build. 34 (2002) 563–572. doi:10.1016/S0378-7788(02)00006-3.
[53] P.O. Fanger, Thermal comfort. Analysis and applications in environmental engineering., Copenhagen: Danish Technical Press., 1970.
[54] ANSI/ASHRAE, ANSI/ASHRAE Standard 55-2017: Thermal Environmental Conditions for Human Occupancy, American Society of Heating, Refrigerating and Air-Conditioning Engineers, Atlanta, GA, US, 2017.
[55] E. Arens, T. Hoyt, X. Zhou, L. Huang, H. Zhang, S. Schiavon, Modeling the comfort effects of short-wave solar radiation indoors, Build. Environ. 88 (2015) 3–9. doi:10.1016/j.buildenv.2014.09.004.
[56] ANSI/ASHRAE, ANSI/ASHRAE Standard 62.1-2016: Ventilation for Acceptable Indoor Air Quality, American Society of Heating, Refrigerating and Air-Conditioning Engineers, Atlanta, GA, US, 2016.
[57] O.A. Seppänen, W.J. Fisk, M.J. Mendell, Association of Ventilation Rates and CO2 Concentrations with Health andOther Responses in Commercial and Institutional Buildings, Indoor Air. 9 (1999) 226–252. doi:10.1111/j.1600-0668.1999.00003.x.

[58] ASTM, ASTM D6245: Standard Guide for Using Indoor Carbon Dioxide Concentrations to Evaluate Indoor Air Quality and Ventilation, American Society for Testing Materials International, West Conshohacken, PA, 2012.
[59] DOE, Commercial Reference Building, (2010). https://energy.gov/eere/buildings/commercial-reference-buildings (accessed January 18, 2018).
[60] Solemma LLC, DIVA 4.0, (2017). http://solemma.net/ (accessed January 18, 2018).
[61] J.A. Jakubiec, F.R. Christoph, DIVA 2.0: integrating daylight and thermal simulations using Rhinoceros 3D, daysim and energyplus, in: Build. Simul. 2011, international building performance simulation association, Sydney, 2011.
[62] G. Ward, R. Shakespeare, Rendering with Radiance, Morgan Kaufmann, San Francisco, Calif, 1998.
[63] M.S. Roudsari, M. Pak, Ladybug: a parametric environmental plugin for grasshopper to help designers create an environmentally-conscious design, in: BS2013, Chambery, France, 2013. http://www.ibpsa.org/proceedings/BS2013/p_2499.pdf (accessed January 18, 2018).
[64] DOE, EnergyPlus, (2016). https://energyplus.net/downloads (accessed January 18, 2018).
[65] DOE, EnergyPlus Input Output Reference, (2017). https://energyplus.net/sites/all/modules/custom/nrel_custom/pdfs/pdfs_v8.8.0/InputOutputReference.pdf (accessed January 18, 2018).
[66] W.J. Fisk, A.H. Rosenfeld, Estimates of Improved Productivity and Health from Better Indoor Environments, Indoor Air. 7 (1997) 158–172. doi:10.1111/j.1600-0668.1997.t01-1-00002.x.
[67] C.S. Mitchell, J. Zhang, T. Sigsgaard, M. Jantunen, P.J. Lioy, R. Samson, M.H. Karol, Current State of the Science: Health Effects and Indoor Environmental Quality, Environ. Health Perspect. 115 (2007) 958–964.
[68] J.G. Allen, P. MacNaughton, U. Satish, S. Santanam, Environmental Health Perspectives – Associations of Cognitive Function Scores with Carbon Dioxide, Ventilation, and Volatile Organic Compound Exposures in Office Workers: A Controlled Exposure Study of Green and Conventional Office Environments, Environ. Health Perspect. (2016). https://ehp.niehs.nih.gov/15-10037/ (accessed December 15, 2017).
[69] A.P. Gagge, A.P. Fobelets, L.G. Berglund, A standard predictive index of human response to the thermal environment, ASHRAE Trans. 92:2B (1986) 709–31.

Appendix

Below we provide the summary of the spatial analysis (Figure 3) and the related discussion. While Figure 3 represents the spatial distribution of luminous and thermal autonomy, the final step in calculating these metrics is to count which nodes meet the respective thresholds and convert the figure into the percentage of nodes across the analysis area, or the mean percentage of occupied hours over one year. Table 3 summarizes these results, including the percentages of time that a node is above or below the thresholds for overly warm/cool or over/underlit.

Regarding adaptive thermal comfort, the building in Phoenix is overly warm for 52% of the time, whereas the building in Helena is overly warm for only 12% of the time. In contrast, the LM-83-12 results ($ASE_{1,000/250hr}$) indicate that only 14% of the building area in Phoenix is overlit whereas 24% of the building area in Helena is overlit.

***Table* 3.** Summary of the results

	Location	Helena, MT	Phoenix, AZ
	Climate Zone	6B Cold and Dry	2B Hot and Dry
Adaptive Comfort (mean, % of occupied hrs)	Thermal autonomy	25	22
	Overly warm hrs	12	52
	Overly cool hrs	63	26
LM-83-12 (% of analysis area)	$sDA_{300/50\%}$	23	22
	$ASE_{1,000/250hr}$	24	14
(mean, % of occupied hrs)	DA_{300} (basis of sDA)	36	39
UDI (mean, % of occupied hrs)	Overlit hrs > 3,000 lux	8	7
	UDI-a	48	54
	Underlit hrs < 300 lux	44	39

When combining the luminous and thermal results, Helena is simultaneously overly cool (63% of the time, based on adaptive-comfort requirements) and overlit (24% of the area, based on LM-83-12 requirements). This tells us that we cannot easily improve our passive solar strategies without increasing the issue of overlighting/glare, so it is important to explore how to increase solar gain in a way that better distributes and diffuses the light. Perhaps the direct sunlight can be admitted in a way whereby it is absorbed by darker surfaces or distributed throughout the space, to reduce glare while still increasing passive solar heating. To better understand this trade-off relationship, we must determine the hourly occurrence of the various characteristics of luminous and thermal autonomy.

The sDA results in Table 3 show another limitation in the use of annual summary values without hourly occurrences. The percentages of areas meeting sDA requirements are almost identical in both locations (22% in Phoenix and 23% in Helena). Based on these values, a designer may conclude that both locations have similar daylight performances, but this is not necessarily true when considering visual and thermal discomfort together. If designers use only one metric to develop their designs, this would prohibit a deeper understanding of the trade-offs between daylight quantity, visual discomfort, and thermal comfort, thereby making it more difficult for designers to come up with balanced design strategies. This shows the importance of analyzing luminous and thermal autonomy simultaneously and emphasizing the temporal variations in both metrics within a building. Section 5.2 and 5.3 introduce the temporal analysis and visualization methods.